Isı Bilimi ve Tekniği Dergisi, 30, 1, 99-110, 2010
J. of Thermal Science and Technology
©2010 TIBTD Printed in Turkey
ISSN 1300-3615

NATURAL CONVECTION IN A TRIANGULAR CROSS SECTION ROOF UNDER DAYLIGHT CONDITIONS

Haydar KÜÇÜK[*] and Hasan GEDİKLİ[**]
* Gümüşhane University, Mechanical Engineering Department,
29000 Gümüşhane, haydarkucuk@hotmail.com
**Karadeniz Technical University, Department of Mechanical Engineering,
61080 Trabzon, hgedikli@ktu.edu.tr

(Geliş Tarihi: 30. 03. 2009, Kabul Tarihi: 18. 09. 2009)

Abstract: The natural convection is numerically investigated in a roof of triangular cross section under constant heat flux with seven different values depending on daylight on the inclined wall, constant wall temperature on the bottom wall and adiabatic on the vertical wall boundary conditions. Continuity, momentum and energy equations are solved by using finite volume method for laminar, two-dimensional and steady-state regime. Streamlines, isotherms, local and mean Nusselt numbers are presented for AR=0.25, 0.5, 0.75 and 1.0 and Ra=10^3, 10^4, 10^5, 10^6. The amount of heat flux ranges from 163 W/m^2 to 808 W/m^2 depending on daylight and the Prandtl number is chosen as 0.7. It is found out that the aspect ratio and Rayleigh number highly affect the heat transfer on the bottom and inclined walls while heat flux slightly affects.
Keywords: Natural convection, Triangular roof, Heat flux, Finite volume method.

GÜNDÜZ ŞARTLARINDA ÜÇGEN KESİTLİ ÇATIDA DOĞAL TAŞINIM

Özet: Dikey duvarında adyabatik, alt duvarında sabit sıcaklık ve eğik duvarda gün ışığına bağlı olarak yedi farklı sabit ısı akısı sınır şartları altında üçgen kesitli çatıda doğal taşınım sayısal olarak incelenmiştir. Sürekli, laminer ve iki boyutlu durum için süreklilik, momentum ve enerji denklemleri sonlu hacim metodu kullanılarak çözülmüştür. Akım çizgileri, eş sıcaklık eğrileri, yerel ve ortalama Nusselt sayıları AR=0.25, 0.5, 0.75 ve Ra=10^3, 10^4, 10^5, 10^6 için sunulmuştur. Isı akısı gün ışığına bağlı olarak 163 W/m^2 ile 808 W/m^2 arasında değişmiş ve Prandtl sayısı 0.7 olarak alınmıştır. Alt duvar ve eğik duvarda ısı transferinin en-boy oranı ve Rayleigh sayısı tarafından oldukça fazla etkilenirken ısı akısı tarafından hafif şekilde etkilendiği belirlenmiştir.
Anahtar kelimeler: Doğal taşınım, Üçgen çatı, Isı akısı, Sonlu hacim metodu.

NOMENCLATURE

g	Gravitational acceleration [m/s^2]
H	Height of the roof [m]
L	Length of bottom wall [m]
AR	Aspect ratio [=H/L]
n	Normal of the wall surface
Nu	Nusselt number, Eqs. (7-8)
p	Pressure [Pa]
Pr	Prandtl number [$=\upsilon/\alpha$]
q''	Heat flux [W/m^2]
Ra	Rayleigh number, Eq. (6)
T	Temperature [K]
u, v	Velocity components in x- and z-directions [m/s]
x,y	Cartesian coordinates [m]
X	dimensionless Cartesian coordinate [=x/L]

Greek symbols

α	Thermal diffusivity [m^2/s]
β	Thermal expansion coefficient [1/K]
ν	Kinematic viscosity [m^2/s]
ρ	Density [kg/m^3]
θ	Dimensionless temperature, Eq. (5)

Subscripts

b	Bottom wall
c	Cold wall
h	Hot wall
L	Local
m	Mean
r	Right wall (inclined wall)

INTRODUCTION

Triangular enclosures are commonly used in many engineering applications such as roofs of the buildings, solar collectors, cooling of electronic devices and various channels of constructions.

A lot of study has been performed for natural convection in triangular enclosures for various applications. Asan and Namli (2000, 2001) investigated the laminar natural convection in a pitched roof of triangular cross section in summer and winter day boundary conditions. They studied the effect of aspect ratio and Rayleigh number on the flow structure and heat transfer. Their results showed that aspect ratio and Rayleigh number have a profound influence on the temperature and flow field. Also, Varol et al. (2006a) studied laminar natural convection in saltbox roofs in summerlike and winterlike boundary conditions. They found out that heat transfer becomes stronger for winterlike boundary condition than that of summerlike boundary condition. Poulikakos and Bejan (1983) reported a theoretical and numerical study of the fluid mechanics inside a right triangular cavity with a cold upper inclined wall, a warm horizontal bottom wall, and an insulated vertical wall. Moreover, Tzeng et al. (2005), Varol et al. (2006b), Koca et al. (2007), Hajri et al. (2007), Basak et al. (2007), Kent (2009a) and Kent (2009b) investigated the laminar natural convection in the triangular cross-section enclosure for different parameters.

Thermal effects examined by Haese and Teubner (2002) in building attics involving ceiling fans with a symmetrical nature of the flow. Kent et al. (2007) analyzed laminar natural convection in right triangular enclosures for various aspect ratios with different boundary conditions and Rayleigh number. Their results show that both the aspect ratio and the Rayleigh number have a strong influence on the streamline patterns and isotherms. Oztop et al. (2007) investigated laminar natural convection heat transfer in a shed roof with or without eave for summer season. They found out that eave length and aspect ratio are the most effective parameters on the heat transfer for the same Rayleigh number. Also, Akinsete and Coleman (1982), Karyakin et al. (1988), Holtzman et al. (2000) and Ridouane et al. (2005) studied the laminar natural convection in the triangular enclosure which applicable for roof geometry at the different boundary conditions. Basak et al. (2009a) focused the analysis and visualization of heat transfer in entrapped triangular cavities within adjacent square tubes forming a system of practical application especially in pollution control with hot fluid flowing through the stack and entrapped cold fluid confined within the triangular cavities. Basak et al. (2009b) analyzed the natural convection heat flow within triangular cavities using Bejan's heatline concept.

To the best of our knowledge, as a consequence of literature review, it was seen that no study related with constant heat flux with different values depending on daylight has been performed in triangular enclosures. For this reason the present study has concentrated the natural convection heat transfer and fluid flow in triangular roof under the heat flux measured in the summer season in Trabzon, Turkey. The inclined wall has constant heat flux, the vertical wall is adiabatic and the bottom wall has constant temperature (cold wall) boundary conditions. The solar radiation amount was measured with Kip-Zonen Solarimeter as Volt (volt*10^{-3}) and then was converted to heat flux as W/m^2 using its calibration curve. The heat flux ranges from 163 to 808 W/m^2, the aspect ratios are 0.25, 0.5, 0.75 and 1.0 and the Rayleigh numbers are 10^3, 10^4, 10^5 and 10^6.

The physical configuration with boundary conditions, the coordinate system of the problem and the variation of heat flux for the time interval from 8:30 a.m. to 16:30 p.m. are shown in Fig. 1. All the fluid properties are constant except the density which was determined according to the Boussinesq approximation. The effects of the aspect ratio, the Rayleigh number and the heat flux on the heat and the flow field are investigated.

GOVERNING EQUATIONS AND NUMERICAL METHOD

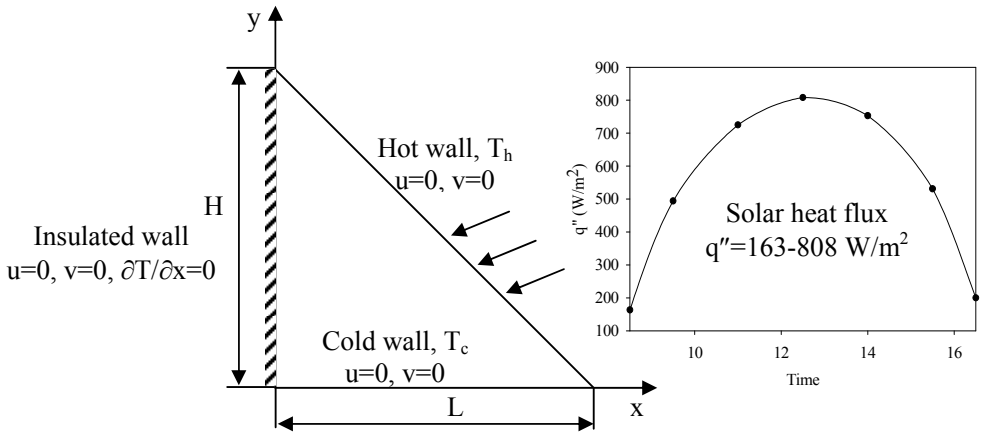

Figure 1. Problem geometry and coordinate system.

The physical configuration and the coordinate system of the problem are shown in Fig. 1 with boundary conditions. The roof was filled with air (Pr=0.7) which is viscous and incompressible Newtonian fluid. The inclined wall (hot wall) exposed to heat flux ranging from 163 to 808 W/m^2, while the bottom wall (cold wall) was kept in constant temperature and the vertical wall was adiabatic. The governing equations for steady, two-dimensional, laminar, incompressible, and Newtonian fluid with Boussinesq approximation (Grey and Giorgini, 1976) for constant fluid properties can be written as:

Continuity Equation

$$\frac{\partial u}{\partial x}+\frac{\partial v}{\partial y}=0 \tag{1}$$

Momentum Equations

$$u\frac{\partial u}{\partial x}+v\frac{\partial u}{\partial y}=-\frac{1}{\rho}\frac{\partial p}{\partial x}+\nu\left(\frac{\partial^2 u}{\partial x^2}+\frac{\partial^2 u}{\partial y^2}\right) \tag{2}$$

$$u\frac{\partial v}{\partial x}+v\frac{\partial v}{\partial y}=-\frac{1}{\rho}\frac{\partial p}{\partial y}+\nu\left(\frac{\partial^2 v}{\partial x^2}+\frac{\partial^2 v}{\partial y^2}\right)+g\beta\left(T-T_c\right) \tag{3}$$

Energy Equation

$$u\frac{\partial T}{\partial x}+v\frac{\partial T}{\partial y}=\alpha\left[\frac{\partial^2 T}{\partial x^2}+\frac{\partial^2 T}{\partial y^2}\right] \tag{4}$$

u = v = 0 on all the walls.
The thermal boundary conditions are:
On the bottom wall T_c = 300, on the inclined wall T_h depends on the heat flux (q″=163-808 W/m^2), and on the vertical wall $\partial T/\partial x=0$.

Dimensionless temperature is defined as

$$\theta=\frac{T-T_c}{T_h-T_c} \tag{5}$$

Rayleigh number is given as

$$Ra=\frac{g\beta\left(T_h-T_c\right)L^3\,\mathrm{Pr}}{\upsilon^2} \tag{6}$$

The local Nusselt numbers can be obtained by an energy balance at the bottom and inclined walls and its expression is given in following:

$$Nu_L=-\left.\frac{\partial\theta}{\partial n}\right|_{wall} \tag{7}$$

The mean Nusselt number can be expressed as

$$Nu_m=\int_s Nu_L\,ds \tag{8}$$

Navier Stokes equations along with the velocity and thermal boundary conditions are solved by Fluent 6.3 commercial software. A segregated solver is adopted with a second order implicit scheme. The SIMPLE method is selected for coupling pressure and velocity and spatial discretizations are done by a second order upwind scheme.

Mesh dependence tests have been conducted based on four meshes as seen in Fig. 2. Based on these tests, the triangular cell with average mesh size of 0.008 (4544 elements) was selected. Also, the relaxation factor is taken as 0.7, 0.7, 1, and 0.3 for u, v, T, and p, respectively. The solutions were assumed to converge when the following convergence criteria was satisfied for every variable at every point in the solution domain

$$\left|\frac{\phi_{new}-\phi_{old}}{\phi_{new}}\right|\le 10^{-4} \tag{9}$$

where ϕ represents u, v and T.

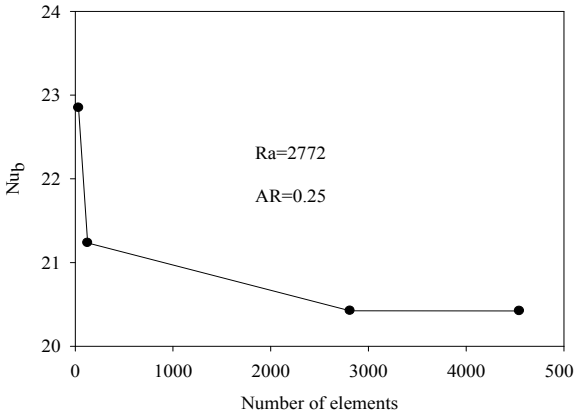

Figure 2. Mesh dependence test.

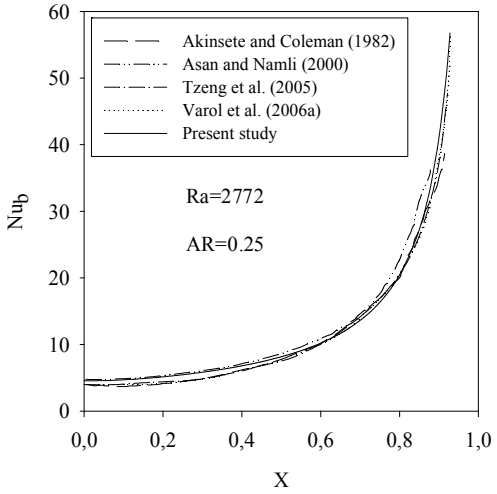

Figure 3. Comparison of local Nusselt number with literature on the bottom wall.

RESULTS AND DISCUSSION

In this study, numerical computations are carried out for AR=0.25, 0.5, 0.75 and 1.0 and Ra=10^3, 10^4, 10^5, 10^6. The amount of heat flux ranges from 163 W/m^2 to 808 W/m^2 depending on daylight and the Prandtl number is chosen as 0.7.

Figs. 4-7 show streamlines (on the left) and isotherms (on the right) for AR=0.25, 0.5, 0.75 and 1.0, respectively. Each figure also represents the effect of Rayleigh number ranging from 10^3 to 10^6 on the flow field and heat transfer. Since the results for all aspect ratios are similar, only the results for AR=1.0 will be discussed for Ra=10^3, 10^4, 10^5 and 10^6. It is seen from the Fig.7 that hot fluid particles near the inclined wall heated by solar heat flux moves upward. Due to the high pressure force occurring near upper side of the triangular enclosure, the fluid is enforced to move downward along the vertical wall to maintain the momentum balance between the buoyancy force and the pressure gradient. Depending on this physical phenomenon a vortex rotating counter-clockwise direction occurs in the roof cross-section. As the streamwise velocity near the walls of the roof is much smaller than that in the gap region because of the no-slip condition, the maximum point of vortex occurs at center of the roof as seen in Fig. 7a (on the left) for Ra=10^3. When the Rayleigh number increases the maximum point of vortex slightly moves towards to upper region of the triangular enclosure and also, the vortex extends towards the intersection of bottom and inclined walls. Moreover, the shape of the vortex changes and its magnitude increases when the Rayleigh number increases. The magnitude of the vortex also increases as the aspect ratio increases. When the Rayleigh number is 10^6 for the AR=1.0 two additional small cells rotating counter-clockwise direction occur inside of the eye of the main vortex. It seems that these additional cells don't occur in the cross-section of the triangular enclosure for the other aspect ratios (AR=0.25, 0.5 and 0.75). For smaller Rayleigh numbers (10^3, 10^4 and 10^5) the effect of the conduction is higher than the convection on the flow field and the heat transfer. When the Rayleigh number increases the convection becomes dominant in the cross section of the triangular roof.

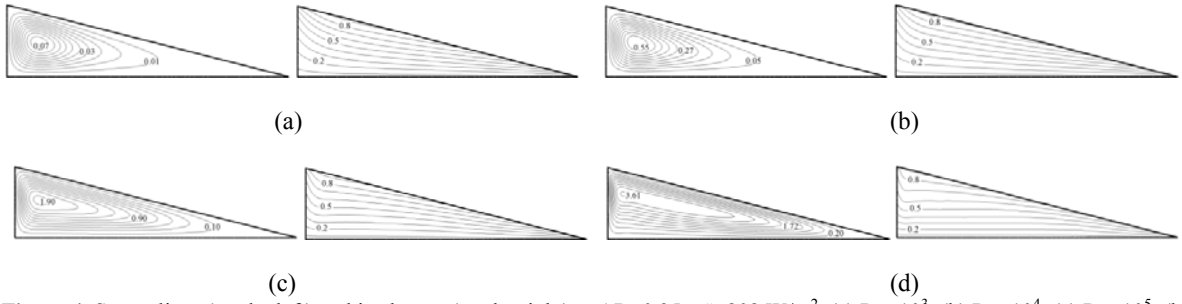

Figure 4. Streamlines (on the left) and isotherms (on the right) at AR=0.25, q″=808 W/m^2, (a) Ra=10^3; (b) Ra=10^4; (c) Ra=10^5; (b) Ra=10^6.

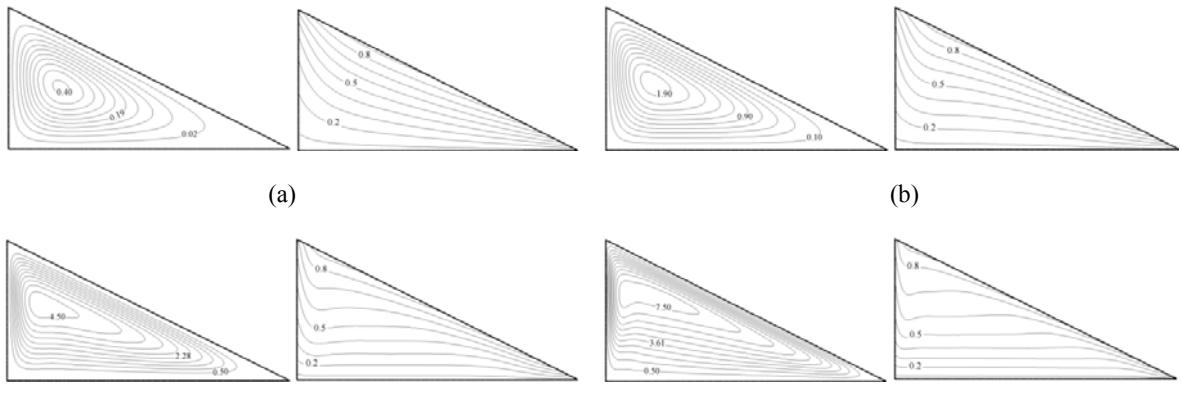

Figure 5. Streamlines (on the left) and isotherms (on the right) at AR=0.5, q″=808 W/m^2, (a) Ra=10^3; (b) Ra=10^4; (c) Ra=10^5; (b) Ra=10^6.

As seen in Figs. 4-7 the forms of isotherms (on the right) change depending on Rayleigh numbers. The isotherms have equal intervals between zero (on the cold bottom wall) and unity (on the region occurring maximum temperature on the inclined wall). It seems that the isotherms appear on the adiabatic vertical wall and tend to intersect to the bottom wall and the inclined wall for small values ($\theta \leq 0.6$). For high values ($\theta > 0.6$) the isotherms emerge from upper side of the inclined wall and move towards to lower side of the inclined wall. When the value of the dimensionless temperature decreases ($\theta \leq 0.6$) the temperature distribution tends to have exponential form. As the Rayleigh number increases (R>10^3) the isotherms near the vertical wall

are enforced towards to the bottom wall. After this point the isotherms have smooth form up to near the inclined wall. It is also observed that when the Rayleigh number increases the smooth form of the isotherm extends to the incline wall. It is seen that this form of the isotherm is directly affected by the flow field (see on the left side of Figs. 4-7). Moreover, when the aspect ratio decreases because of small gap between bottom and inclined walls high temperature gradient occurs in the cross-section of the triangular enclosure. Especially, on the intersection of bottom and inclined walls high temperature gradient takes place because these walls are very close to each other (see on the right side of Figs. 4-7).

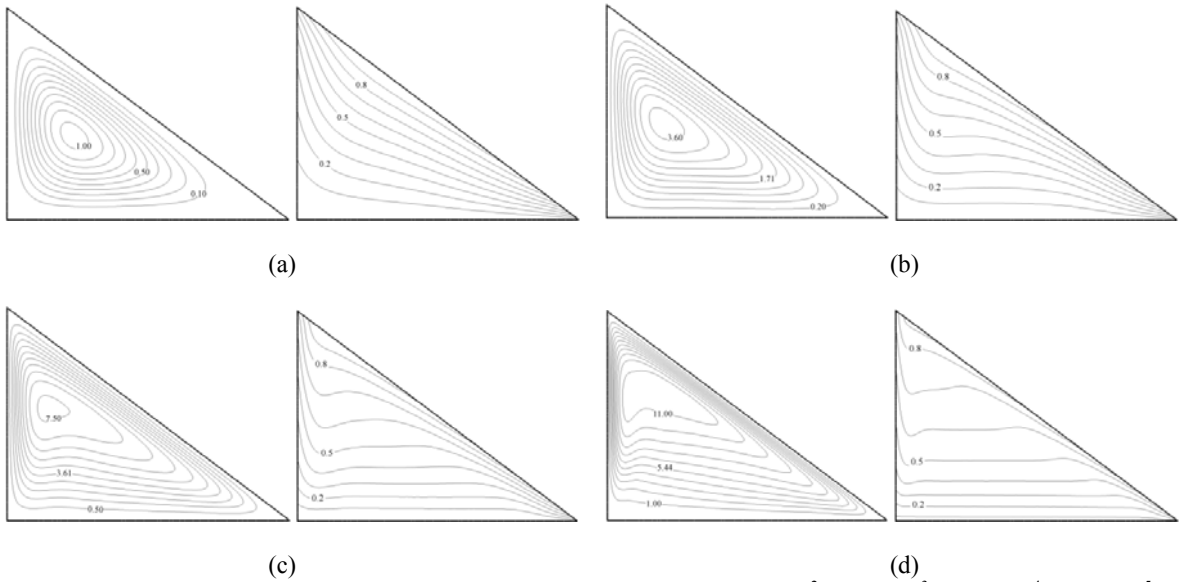

(a) (b)

(c) (d)

Figure 6. Streamlines (on the left) and isotherms (on the right) at AR=0.75, q″=808 W/m^2, (a) Ra=10^3; (b) Ra=10^4; (c) Ra=10^5; (b) Ra=10^6.

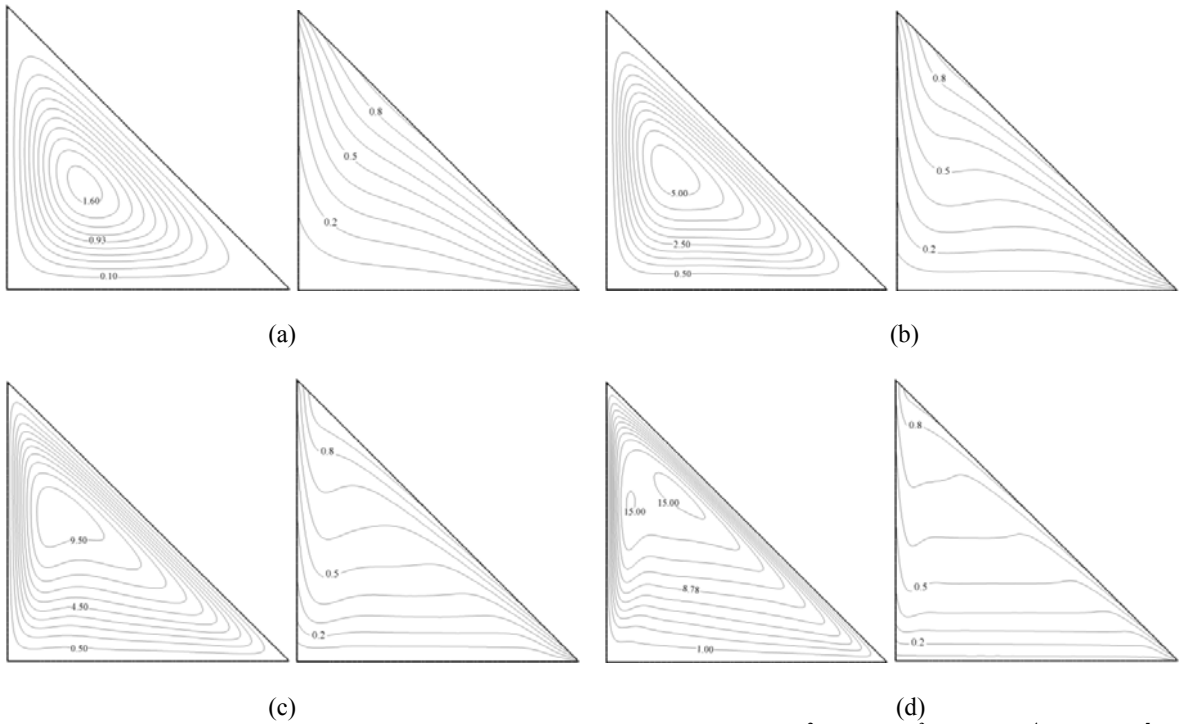

(a) (b)

(c) (d)

Figure 7. Streamlines (on the left) and isotherms (on the right) at AR=1.0, q″=808 W/m^2, (a) Ra=10^3; (b) Ra=10^4; (c) Ra=10^5; (b) Ra=10^6.

The variation of local Nusselt number with Rayleigh number on the bottom wall for q″=808 W/m^2 are presented in Figs. 8a-d for the aspect ratios of AR=0.25, 0.5, 0.75 and 1.0, respectively. It is observed that when the Rayleigh number increases the local Nusselt number increases on the left side of the bottom wall. Contrary to

this, on the right side of the bottom wall as the Rayleigh number increases the local Nusselt number decreases. The transition point occurs about between X=0.1 and X=0.5 for AR=0.25. The transition point moves towards the right side of the bottom wall when the aspect ratio and Rayleigh number increases. It is clearly shown that when the Rayleigh number is high ($Ra=10^6$) the local Nusselt number almost constant between X=0.01 and X=0.6 for AR=0.25 along the bottom wall. Moreover, it seems that when the aspect ratio increases the constant value region extends and the constant local Nusselt value regions occur for low Rayleigh number ($Ra\leq10^5$). For all Rayleigh number and aspect ratios highest temperature gradient occurs near the edges of the bottom wall because of small gap between cold and hot walls. Therefore, most of the heat transfer across the base wall occurs near the intersection between the bottom and inclined walls. It is found that the highest local Nusselt number occurs in the triangular enclosure with AR=0.25 and when the aspect ratio increases the local Nusselt number decreases.

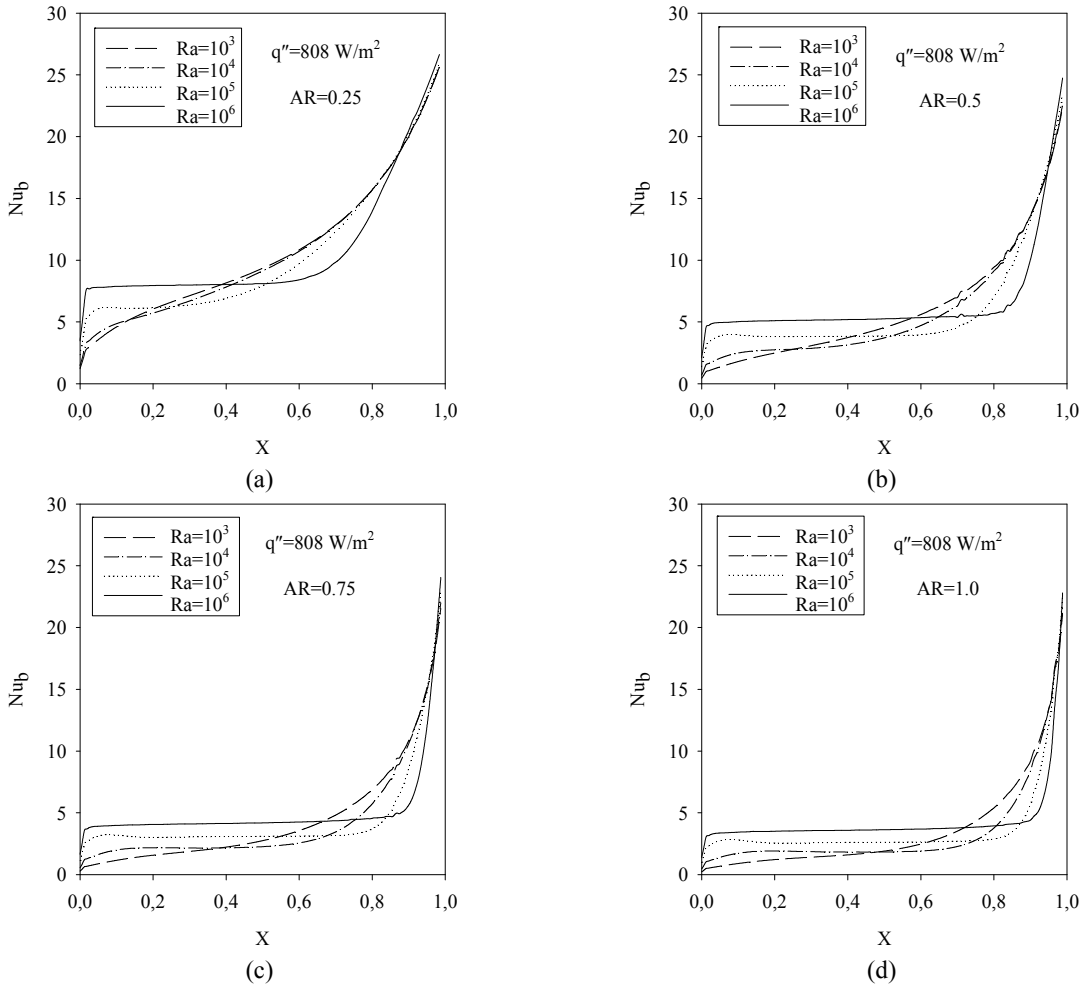

Figure 8. Variation of local Nusselt number with dimensionless length for different Rayleigh number on bottom wall, (a) AR=0.25; (b) AR=0.5; (c) AR=0.75; (d) AR=1.0

The variation of local Nu with Ra on the inclined (right) wall for $q''=808$ W/m^2 are presented in Figs. 9a-d for the aspect ratio of AR=0.25, 0.5, 0.75 and 1.0, respectively. It is seen from these figures that when the Rayleigh number increases the local Nusselt number decreases on the nearby region of the intersection of the inclined and the vertical walls. Whereas, after X=0.2 as the Rayleigh number increases the local Nusselt number increases. Between X=0 and X=0.2 the local Nusselt number decreases and then increases along the inclined wall and reaches the maximum value the near intersection of the bottom and the inclined wall because of high temperature gradient. For aspect ratio of AR=0.25 the local Nu is almost the same for $Ra=10^3$ and $Ra=10^4$. It is also observed that the differences between local Nusselt numbers increase when the Rayleigh number increases with the increasing aspect ratio. It seems that for $Ra\leq10^4$ the local Nusselt numbers slightly increase when the aspect ratio increases between X=0.2 and X=0.8. Moreover, it is found out that local Nusselt number obtained on the inclined wall (Fig. 9) is highly higher than that of the bottom wall (Fig. 8).

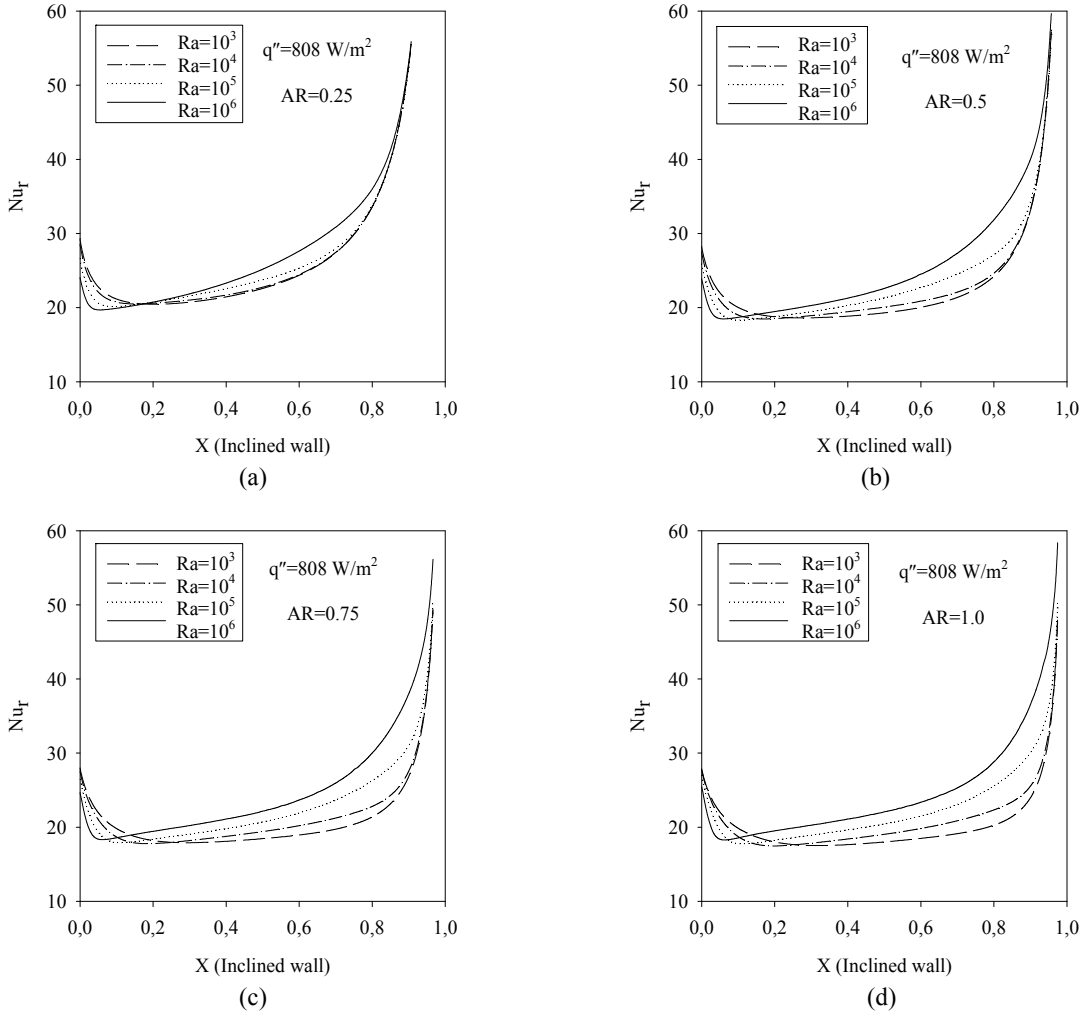

Figure 9. Variation of local Nusselt number with dimensionless length for different Rayleigh number on right wall, (a) AR=0.25; (b) AR=0.5; (c) AR=0.75; (d) AR=1.0

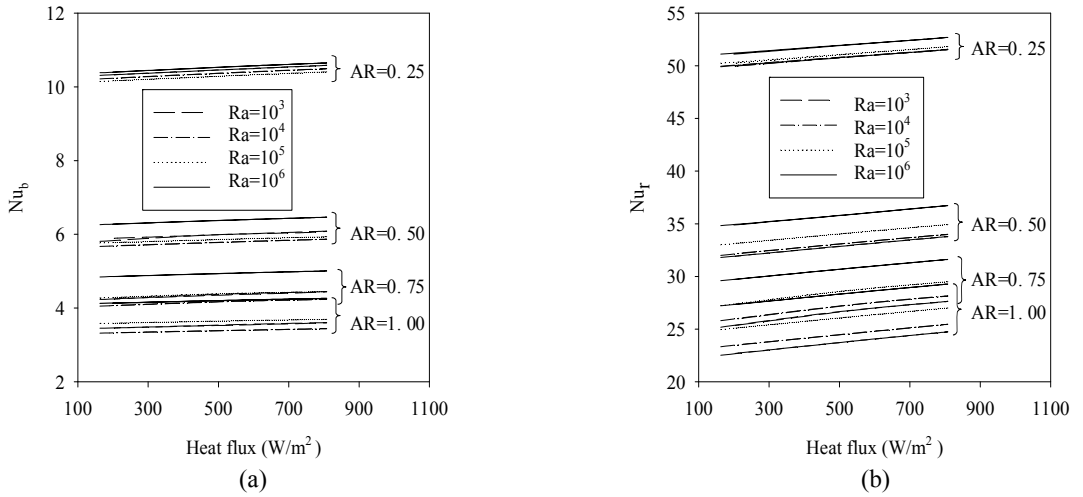

Figure 10. Variation of mean Nusselt number with time for different Rayleigh number and different aspect ratio, (a) bottom wall; (b) right wall

Figs. 10a and b represent the variation of mean Nusselt number with heat flux on the bottom and the inclined wall, respectively. It seems that the mean Nusselt number changes depending on the amount of solar heat flux, Rayleigh number and the aspect ratio on both the bottom and the inclined walls. When the heat flux increases the mean Nusselt number increases on both walls. It is seen that the increasing of mean Nusselt

number with heat flux on the inclined wall is higher than that of the bottom wall. As seen from isotherms maximum point of inclined wall temperature tends to upper corner and hot fluid particles are forced to upwards by buoyancy force. So, when the heat flux highly increases the temperature gradient slightly increases. Also, in the triangular enclosures heated from the top the conduction heat transfer is dominant. So, although increasing of heat flux is quite high, increasing of heat transfer is limited in the triangular enclosures. The highest value of the mean Nusselt number is obtained in the roof with the lowest aspect ratio due to the short distance between hot and cold walls. As the aspect ratio increases the mean Nusselt number decreases. Furthermore, it is found that the mean Nusselt number obtained on the inclined wall is much higher than that of the bottom wall as expected because high temperature gradient. It is also shown that the highest mean Nusselt number obtained on the bottom and the inclined walls for AR=0.25 depends on the local Nusselt number. As the aspect ratio increases the mean Nusselt number decreases on the each wall. As seen from Fig.10a, the highest values for the mean Nusselt number on the bottom wall are obtained for $Ra=10^6$, 10^3, 10^4 and 10^5, in descending order. It is also seen that their values are very close to each other. The effect of the conduction on the heat transfer is higher than the convection due to the quasi-conduction regime in the triangular enclosure with the lowest aspect ratio. When the aspect ratio is 0.5 the highest values of the mean Nusselt number occur for $Ra=10^6$, 10^3, 10^5 and 10^4, in descending order. When AR=0.75 and 1.0 the highest values of the mean Nu are obtained for $Ra=10^6$, 10^5, 10^3 and 10^4, in descending order. It is observed in Fig. 10a that the mean Nu values are close to each other for small Rayleigh number ($Ra\leq10^5$) at each aspect ratio due to the quasi-conduction regime. It is seen that as the aspect ratio increases the effect of the Rayleigh number increases on heat transfer especially for $Ra=10^6$. Fig 10b shows that when the Rayleigh number increases the mean Nusselt number increases on the inclined wall. It is observed that for AR≥0.5 the effect of convection on the heat transfer increases when the aspect ratio increases for $Ra>10^5$ both on bottom and inclined walls. For small Rayleigh number the mean Nusselt numbers are close to each other on the inclined wall similar to those of the bottom wall due to the dominant conduction regime.

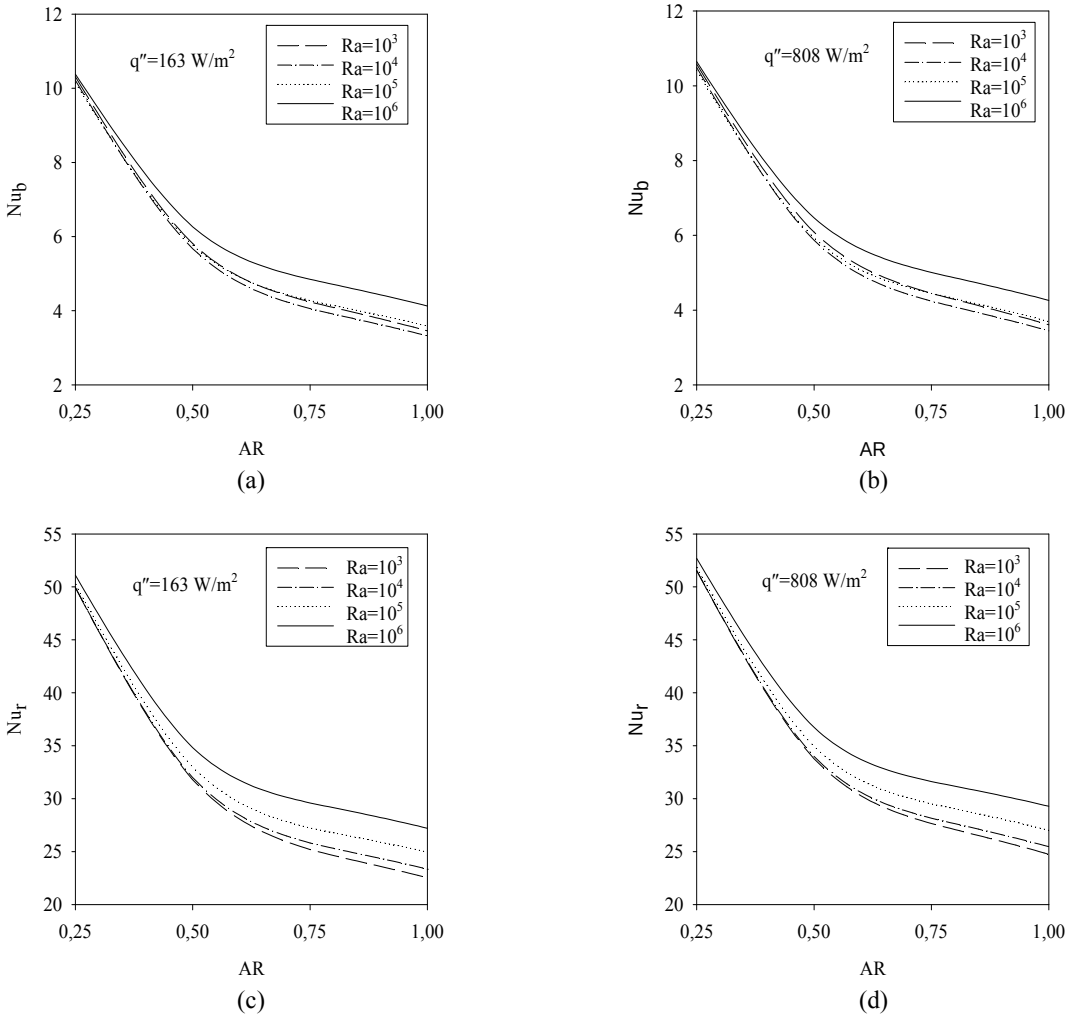

Figure 11. Variation of mean Nusselt number with aspect ratio, (a,b) bottom wall; (c,d) right wall.

The variation of the mean Nusselt number with the aspect ratio for different Rayleigh number are presented in Figs. 11a and b (on the bottom wall) and Figs. 11c and d for the inclined wall at q″=163 W/m^2 and q″=808 W/m^2. It is seen from these figures that the mean Nusselt number highly decreases as aspect ratio increases because of high gap between bottom and inclined walls. It is observed that for Ra≤10^5 the values for the mean Nusselt numbers are close to each other because of dominant conduction regime in the cross-section of the triangular roof. The mean Nu highly increases due to the dominant convection regime in the cross-section of the triangular enclosure for Ra=10^6. Also, it seems that when the heat flux increases the mean Nu slightly increases on the bottom and inclined walls because the conduction heat transfer is dominant in the triangular enclosures heated from the top. It is shown that the mean Nu obtained on the inclined wall is clearly higher than that of the bottom wall because the high temperature gradient. It is seen that when the Rayleigh number increases the mean Nusselt number increases on the inclined wall.

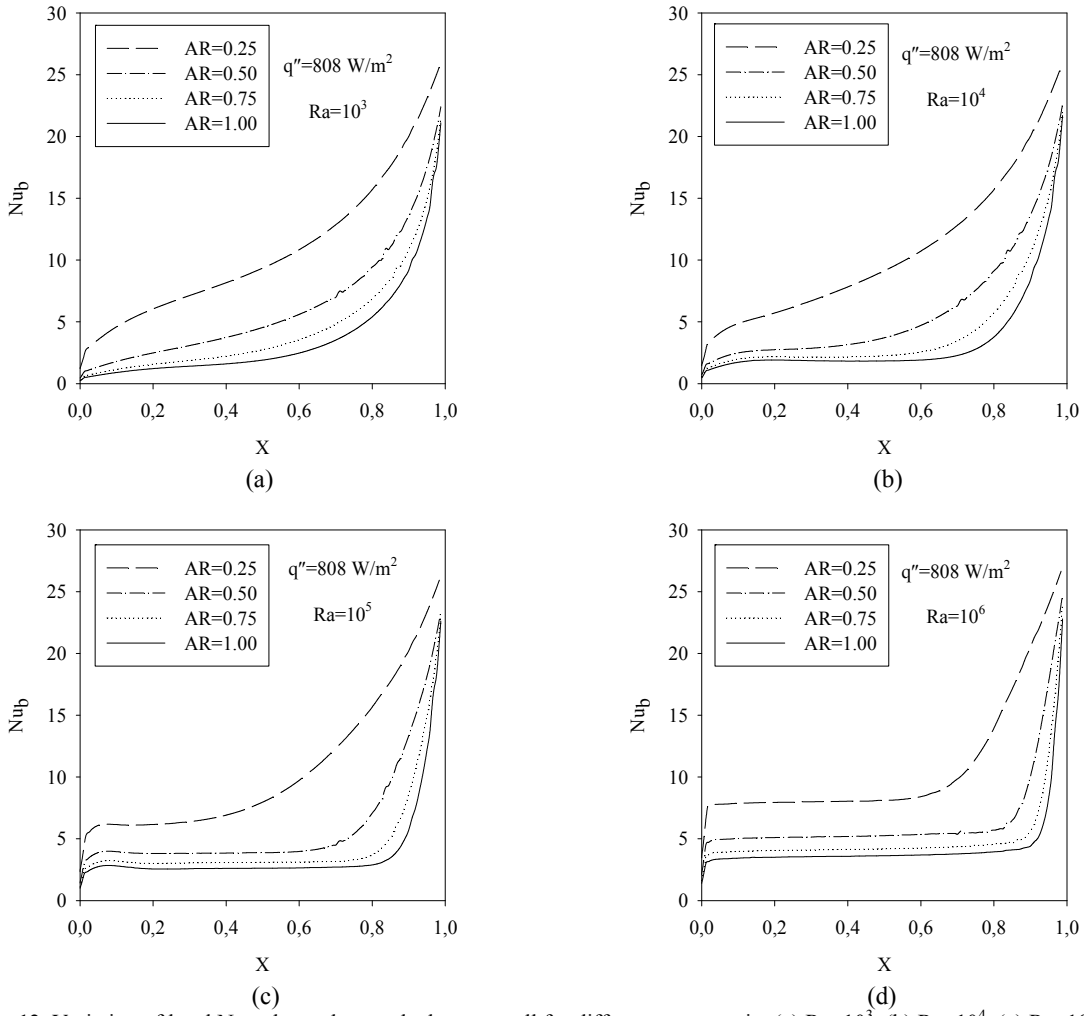

Figure 12. Variation of local Nusselt number on the bottom wall for different aspect ratio, (a) Ra=10^3; (b) Ra=10^4; (c) Ra=10^5; (d) Ra=10^6.

The variation of the local Nusselt number along the bottom wall are shown in Figs. 12a-d for Ra=10^3, 10^4, 10^5 and 10^6, respectively. It is shown that the highest local Nusselt number occurs in the triangular roof with the lowest aspect ratio (AR=0.25) and when the aspect ratio increases the local Nusselt number decreases. Also, it is observed that the lowest local Nusselt number is obtained on the intersection of the vertical and the bottom walls. Then the local Nusselt number increases along the bottom wall for Ra≤10^4 (conduction is dominant in the cross-section of the triangular roof). Moreover, it is found out that when the Rayleigh number increases the local Nusselt number becomes almost constant on the bottom wall especially for Ra>10^4 (convection is dominant in the cross-section of the triangular enclosure).

Figs. 13a-d show the variation of the local Nusselt number along the inclined wall for Ra=10^3, 10^4, 10^5 and 10^6, respectively. It is seen that near to the intersection of the vertical and the inclined walls the local Nusselt number decreases and the Nu number are almost the same for all the aspect ratios. After X=0.2 the local Nusselt number increases along the inclined wall and

reaches maximum value near to the intersection of the bottom and the inclined walls because of high temperature gradient. The highest values of the local Nusselt number occur in the triangular roof at the lowest aspect ratio (AR=0.25) because of lowest gap between hot and cold wall. When the aspect ratio increases the mean Nusselt number decreases. It is also, it shown that the values for the local Nusselt number are close to each other especially for $Ra \geq 10^4$ except AR=0.25. The differences between the local Nusselt numbers for all aspect ratios decrease when the Rayleigh number increases.

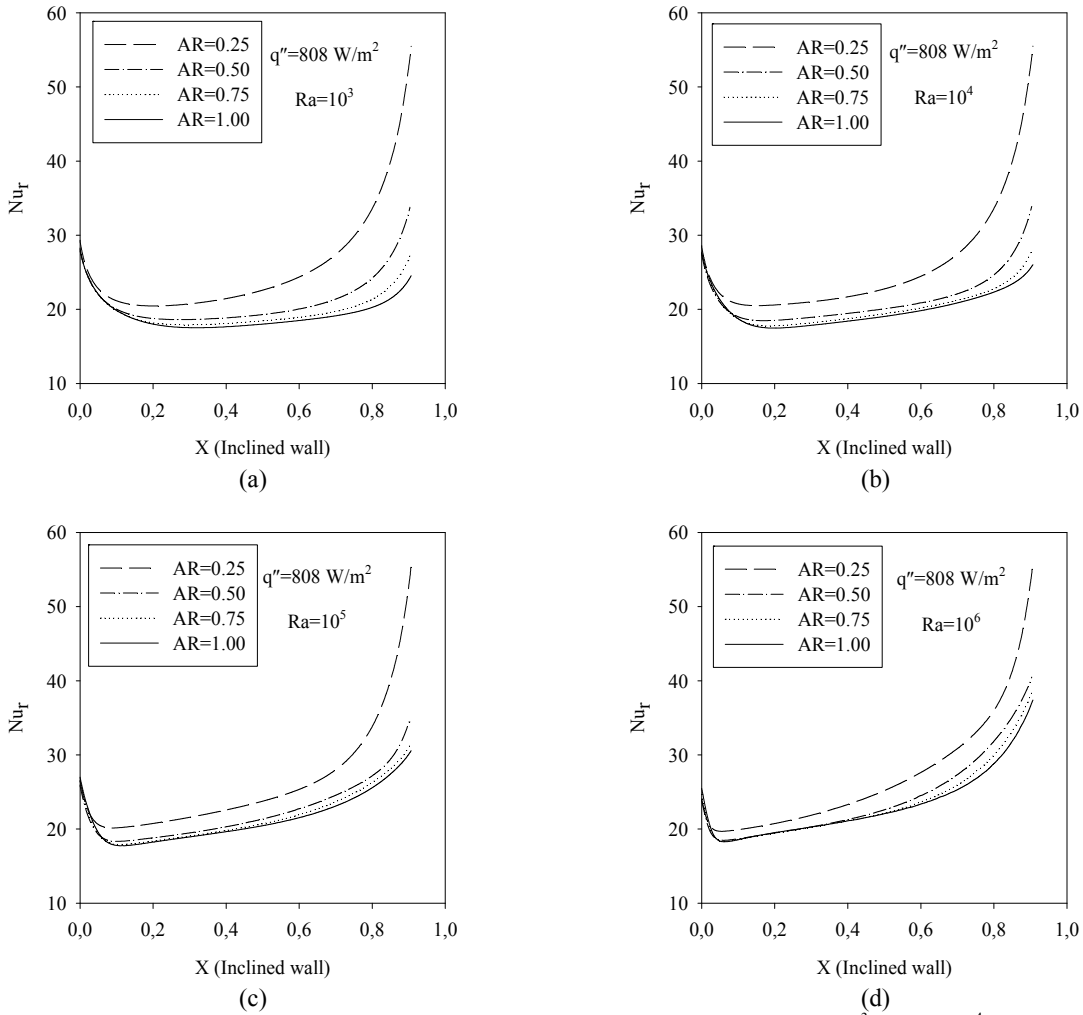

Figure 13. Variation of local Nusselt number on the right wall for different aspect ratio, (a) $Ra=10^3$; (b) $Ra=10^4$; (c) $Ra=10^5$; (d) $Ra=10^6$.

Figs. 14a and b present the variation of the mean Nusselt number with the Rayleigh number on the bottom wall for q″=163 W/m^2 and for q″=808 W/m^2, respectively. Also, Figs. 14c-d show the same variation on the inclined wall for the same amounts of the heat flux. It is seen that the highest value of mean Nusselt number occur in the triangular roof with the lowest aspect ratio because of short distance between hot and cold walls. So, when the aspect ratio increases the mean Nusselt number decreases. It is shown that the mean Nusselt number changes very slightly when the Rayleigh number and the amount of the heat flux increase because of the conduction dominant heat transfer mechanism in the triangular enclosures heated from the top. This increase is more pronounced for the higher aspect ratios than the lower aspect ratios. Furthermore, it is found that the mean Nusselt number obtained on the inclined wall is much higher than that of the bottom wall because of high temperature gradient.

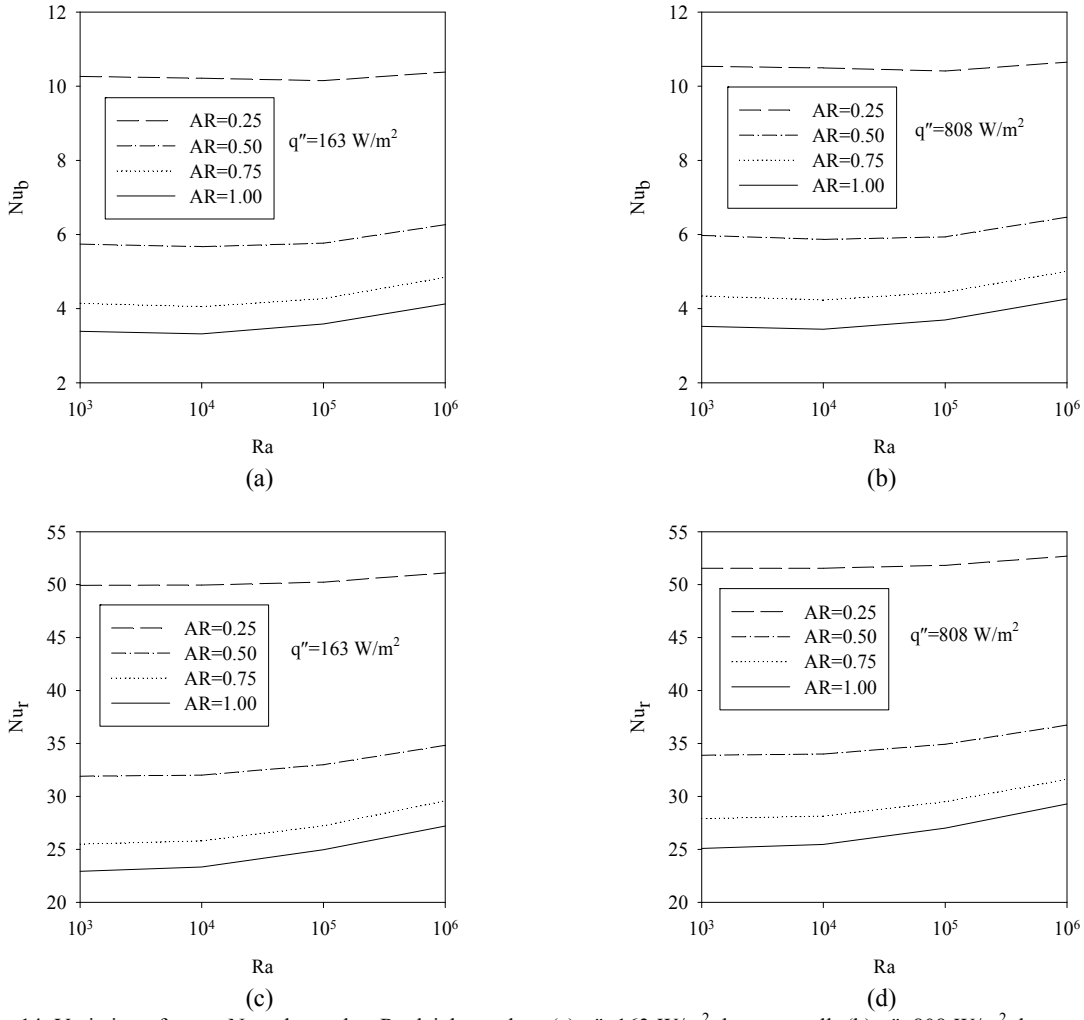

Figure 14. Variation of mean Nusselt number Rayleigh number, (a) q″=163 W/m^2, bottom wall; (b) q″=808 W/m^2, bottom wall; (c) q″=163 W/m^2, right wall; (d) q″=808 W/m^2, right wall.

CONCLUSIONS

This study reports the natural convection heat transfer and the fluid flow in triangular enclosure under heat flux on the inclined wall during daylight of the summer season in Trabzon, Turkey. The effective parameters such as the amount of solar heat flux, the aspect ratio and the Rayleigh number on the flow field and the heat transfer are numerically investigated.

A vortex rotating counter-clockwise direction occurs in the roof cross-section and the maximum point of vortex occurs at center of the cross-section of the roof. When the Rayleigh number increases, the maximum point of vortex slightly moves towards to the upper region of the triangular enclosure and the local Nusselt number increases on the left side and decreases on the right side of the bottom wall. Also, as the Rayleigh number increases the local Nu number decreases on the left side and increases on the right side of the inclined wall. The mean Nusselt number changes depending on the aspect ratio, the Rayleigh number and the heat flux.

The most effective factors on the heat transfer are found to be the aspect ratio, Rayleigh number and heat flux, in descending order. The highest value of the mean Nu occurs in the roof at the lowest aspect ratio. When the aspect ratio increases the mean Nusselt number highly decreases. When the heat flux increases the mean Nusselt number slightly increases on both the bottom and the inclined walls. The mean Nu obtained on the inclined wall is much higher than that of the bottom wall. For Ra>10^5 and AR≥0.5 the effect of convection becomes dominant in the cross-section of triangular roof.

REFERENCES

Akinsete, V. and Coleman, T.A., Heat Transfer by Steady Laminar Free Convection in Triangular Enclosures, *Int. J. Heat Mass Transfer* 25, 991-998, 1982.

Asan, H. and Namli, L., Laminar Natural Convection in a Pitched Roof of Triangular Cross-Section: Summer Day Boundary Conditions, *Energy and Buildings* 33, 69–73, 2000.

Asan, H. and Namli, L., Numerical Simulation of Buoyant Flow in a Roof of Triangular Cross Section under Winter Day Boundary Conditions, *Energy and Buildings* 33, 753–757, 2001.

Basak, T., Roy, S. and Thirumalesha, Ch., Finite Element Analysis of Natural Convection in a Triangular Enclosure: Effects of Various Thermal Boundary Conditions, *Chemical Engineering Science* 62, 2623-2640, 2007.

Basak, T., Roy, S. and Aravind, G., Analysis of Heat Recovery and Thermal Transport within Entrapped Fluid Based on Heatline Approach, *Chemical Engineering Science* 64(8), 1673-1686, 2009a.

Basak, T., Aravind, G. and Roy, S., Visualization of Heat Flow due to Natural Convection within Triangular Cavities Using Bejan's Heatline Concept. *Int. J. Heat and Mass Transfer* 52(11-12), 2824-2833, 2009b.

Gray, D. D. and Giorgini, A., The Validity of the Boussinesq Approximation for Liquids and Gases, *Int. J. Heat Mass Transfer* 19, 545-551, 1976.

Haese, P.M. and Teubner M.D., Heat Exchange in an Attic Space, *Int. J. Heat Mass Transfer* 45, 4925-4936. 2002.

Hajri, I., Omri, A. and Nasrallah S. B., A Numerical Model for the Simulation of Double-Diffusive Natural Convection in a Triangular Cavity Using Equal Order and Control Volume Based on the Finite Element Method, *Desalination* 206, 579-588, 2007.

Holtzman, G. A., Hill, R. W. and Ball, K. S., Laminar Natural Convection in Isosceles Triangular Enclosures Heated from Below and Symmetrically Cooled from Above, *J. Heat Transfer* 122, 485-491, 2000.

Karyakin, Y. E., Sokovishin, Y. A. and Martynenko, O. G., Transient Natural Convection in triangular enclosures, *Int. J. Heat Mass Transfer* 31, 1759-1766, 1988.

Kent, E. F., Asmaz, E. and Ozerbay, S., Laminar Natural Convection in Right Triangular Enclosures, *Heat Mass Transfer* 44, 187-200, 2007.

Kent, E. F., Numerical Analysis of Laminar Natural Convection in Isosceles Triangular Enclosures, *Proc. IMechE Part C: J. Mechanical Engineering Science* 223(5), 1157-1169, 2009a.

Kent, E. F., Numerical Analysis of Laminar Natural Convection in Isosceles Triangular Enclosures for Cold Base and Hot Inclined Walls, *Mechanics Research Communications* 36(4), 497-508, 2009b.

Koca, A., Oztop, H. F. and Varol, Y., The Effects of Prandtl Number on Natural Convection in Triangular Enclosures with Localized Heating from Below, *Int. Commun. Heat and Mass Transfer* 34, 511-519, 2007.

Oztop, H. F., Varol, Y. and Koca, A., Laminar Natural Convection Heat Transfer in a Shed Roof with or without Eave for Summer Season, *Applied Thermal Engineering* 27, 2252-2265, 2007.

Poulikakos, D. and Bejan, A., The Fluid Mechanics of an Attic Space, *J. Fluid Mechanics* 131, 251-269, 1983.

Ridouane, E. H., Campo, A. and McGarry, M., Numerical Computation of Buoyant Airflows Confined to Attic Spaces under Opposing Hot and Cold Wall Conditions, *Int. J. Thermal Science* 44, 944-952, 2005.

Tzeng, S. C., Liou, J. H. and Jou, R. Y., Numerical Simulation-Aided Parametric Analysis of Natural Convection in a Roof of Triangular Enclosures, *Heat Transfer Engineering* 26, 69–79, 2005.

Varol, Y., Koca, A. and Oztop, H. F., Laminar Natural Convection in Saltbox Roofs for both Summerlike and Winterlike Boundary Conditions, *Journal of Applied Sciences* 6 (12), 2617-2622, 2006a.

Varol, Y., Koca, A. and Oztop, H. F., Natural Convection in a Triangle Enclosure with Flush Mounted Heater on the Wall, *Int. Commun. Heat Mass and Transfer* 33, 951–958, 2006b.

Haydar Küçük is an assistant professor at Gümüşhane University, Gümüşhane, Turkey. He received his Ph.D. in 2003 from Karadeniz Technical University. His research interests involve numerical heat transfer and fluid flow, drying and drying models, energy and exergy analyses. He has published 18 articles in recognized journals and proceedings.

Hasan Gedikli is an assistant professor at Karadeniz Technical University, Trabzon, Turkey He received his Ph.D. in 2005 from Karadeniz Technical University. His research interests involve the finite element modeling and analysis, metal forming, impact and fluid-structure interaction. He has published 11 articles in recognized journals and proceedings.